Quantitating the Dynamics of NBD Hexanoic Acid in Homogeneous Solution and in Solutions Containing Unilamellar Vesicles

Kelly P. Greenough and G. J. Blanchard*

Department of Chemistry, Michigan State University, East Lansing, Michigan 48824-1322

Received: December 5, 2005; In Final Form: February 1, 2006

We report here on the motional and fluorescence lifetime dynamics of the chromophore NBDHA (6-(*N*-(7-nitrobenz-2-oxa-1,3-diazol-4-yl)amino)hexanoic acid) in neat solvents and in aqueous solutions containing unilamellar vesicles of varying composition. We measure the transient response of this chromophore by time-correlated single-photon counting, using one- and two-photon excitation to resolve the Cartesian components of the rotational diffusion constant, *D*. Our experimental data for NBDHA in selected solvents of varying viscosity demonstrate that one- and two-photon excitation probe different components of the rotational diffusion constant and that this chromophore reorients as a prolate rotor with an aspect ratio of ∼2. For NBDHA in aqueous solutions containing unilamellar vesicles of varying composition, we recover the same reorientation behavior regardless of vesicle composition. Fluorescence lifetime and steady-state fluorescence data show the chromophore to reside in a polar environment that is different from neat water. We understand these data in the context of the chromophore residing in close proximity to the unilamellar vesicle polar headgroups in all cases.

Introduction

Lipid bilayers have attracted a great deal of attention because of the central role these structures play in mediating life processes. As our understanding of these structures has improved, it has become clear that plasma membranes are exceedingly complex heterogeneous structures comprised of multiple different constituents, with the relative amount of each depending on the function of the cell. Early work on understanding plasma membranes pointed to the existence of some bilayer constituents that were not detergent-soluble, and more detailed analysis of these insoluble fractions revealed that they were enriched in cholesterol content. This finding, combined with work on multicomponent model bilayer systems, led to the notion that "lipid rafts" may exist in cellular membranes.[1] Such rafts are thought to be regions of locally high cholesterol concentration, with sphingolipids playing a supportive role in raft formation owing to the ability of this family of lipids to hydrogen bond. While there is abundant evidence in the literature for phase separation in two- and three-component bilayer model systems,[2−4] the existence of lipid rafts in plasma membranes remains to be established firmly.

We are interested in biomimetic lipid bilayer structures because of the possibility that these structures can be used to support transmembrane proteins in their active forms. A first step in this work is to understand the local environments formed by model bilayer structures as a function of their composition. To gain information on these heterogeneous systems from a molecular perspective, we are interested in imbedding selected chromophores in these structures. In this paper, we report on the optical properties of the chromophore NBDHA (6-(*N*-(7-nitrobenz-2-oxa-1,3-diazol-4-yl)amino)hexanoic acid). The NBD chromophore is used widely for investigations of bilayer systems, and we focus here on the details of chromophore motion both in neat solvents and in solutions containing unilamellar vesicles. We have chosen to study the hexanoic acid derivative of this chromophore in an effort to understand where in the unilamellar vesicle structures such an amphiphilic chromophore will reside. Our specific choice of a chromophore possessing an amphiphilic side group that differs in structure from either the phospholipid or cholesterol bilayer constituents was deliberate. We are interested in understanding both polarity-mediated and structurally mediated interactions within lipid bilayers, and this work centers on polarity-mediated interactions. We have chosen to use an NBD derivative because of the extensive knowledge base that already exists for this chromophore.[5−11] Our data in neat solvents reveal that NBDHA reorients as a prolate rotor with an aspect ratio $D_z/D_x \sim 2$. For NBDHA in vesicle-containing solutions, we find that the chromophore experiences the same environment regardless of vesicle composition or the specific phospholipid used. This finding, in conjunction with steady-state absorbance and emission data, and fluorescence lifetime data, points to the NBDHA residing in close proximity to the headgroup region of the vesicles. Because the pK_a of NBDHA is ca. 4.5 and the aqueous vesicle solutions are buffered to pH 8, the chromophore exists in a predominantly deprotonated (anionic) form, facilitating association with the phosphocholine headgroups of the lipids.

Experimental Section

Materials. The fluorescent probe 6-(*N*-(7-nitrobenz-2-oxa-1,3-diazol-4-yl)amino)hexanoic acid (NBDHA) was obtained from Molecular Probes, Inc., and used without further purification. The solvents methanol, 1-propanol, 1-butanol, 1-pentanol, dimethyl sulfoxide (DMSO), *N*,*N*-dimethylformamide (DMF), and acetonitrile were purchased from Sigma-Aldrich in their highest purity available. Water and ethanol (95%) were distilled in-house. For time-resolved fluorescence measurements, the concentration of NBDHA in solvents and the concentration of NBDHA in the vesicles for one-photon experiments was 10^{-5}

* To whom correspondence should be addressed. E-mail: blanchard@chemistry.msu.edu.

10.1021/jp057073v CCC: $33.50
Published on Web 03/08/2006

M, while the concentration of NBDHA in vesicles for two-photon experiments was 10^{-4} M.

For the construction of unilamellar vesicles, the lipids 1,2-dilauroyl-*sn*-glycero-3-phosphocholine (DLPC, mp = −1 °C), 1,2-distearoyl-*sn*-glycero-3-phosphocholine (DSPC, mp = 55 °C), egg sphingomyelin (SPM), and powdered cholesterol were obtained from Avanti Polar Lipids, Inc. Although DLPC and DSPC are not major components of plasma membranes, they were chosen based on their significant difference in transition temperatures. The vesicle constituents were prepared in a 1:1:1 mole ratio of phospholipid/cholesterol/sphingomyelin or a 2:1 mole ratio of phospholipid/cholesterol for the multicomponent systems. For the mixed lipid systems, the ratio of phospholipids used was 1:1. A total of nine vesicle systems were produced with varying composition. The vesicle compositions were as follows: DLPC, DLPC/cholesterol, DLPC/cholesterol/SPM, DSPC, DSPC/cholesterol, DSPC/cholesterol/SPM, DLPC/DSPC, DLPC/DSPC/cholesterol, and DLPC/DSPC/cholesterol/SPM. Chloroform was evaporated from the lipid solutions, then the vesicle constituents were dissolved in a 4:1 benzene/methanol solvent system, followed by another evaporation. The resulting lipid mixture was then dissolved in a 10 mM solution of Tris buffer (Aldrich) in Milli-Q water. The Tris buffer was adjusted for a pH ∼8. An equal volume of the NBDHA-containing solution (2×10^{-4} M) was added next for a final total concentration of the vesicle constituents of 1 mg/mL and 10^{-4} M in NBDHA. This probe concentration corresponds to ∼7000 chromophore molecules per 100 nm diameter vesicle. The average distance between chromophores is calculated to be ∼30 Å, a distance that could give rise to efficient Förster excitation transport. To test for this possibility, we compared our time-resolved and steady-state data for 10^{-4} M solutions to the same data for 10^{-5} M solutions and found that they were identical to within the experimental uncertainty.

We used the extrusion method[12−15] to produce small unilamellar vesicles of approximately 100 nm diameter. The lipid suspensions experienced five freeze−thaw−vortex cycles to aid in mixing of the constituents. The suspensions were frozen in liquid nitrogen for 5 min, followed by thawing in a hot water bath (5 min), then vortexed for approximately 2 min. For vesicle formation, a syringe-based miniextruder from Avanti Lipids, Inc., was used. The lipid suspension was extruded 11 times through a polycarbonate filter with 100 nm diameter pores to produce vesicles. Transmission electron microscopy (TEM) measurements were used to verify vesicle size following extrusion.

Steady-State Measurements. All absorption spectra were recorded on a Cary model 300 double beam UV−visible absorption spectrophotometer, with 1 nm spectral resolution. All emission spectra were recorded on a Spex Fluorolog 3 spectrometer at a spectral resolution of 3 nm for both excitation and emission monochromators.

Time-Correlated Single Photon Counting Measurements. All lifetime and anisotropy measurements of solvent and vesicle solutions were collected using a time-correlated single photon counting (TCSPC) system. This system has been described in detail elsewhere and we provide only a brief recap of its salient features here. The source laser is a continuous wave mode-locked Nd:YAG laser (Coherent Antares 76-S) that produces 100 ps 1064 nm pulses at a 76 MHz repetition rate. The second or third harmonic of the output of this laser is used to excite a cavity dumped dye laser (Coherent 702-2), operating with Rhodamine 610 dye (Exciton, 532 nm pump) for two photon excitation experiments, or with Stilbene 420 dye (Exciton, 355 nm pump) for one-photon excitation experiments. The dye laser outputs were 5 ps pulses at a repetition rate of 4 MHz for both excitation wavelengths. Fluorescence signals were detected using a Hamamatsu R3809U microchannel plate photomultiplier tube detector with a Tennelec 454 quad constant fraction discriminator and Tennelec 864 time-to-amplitude converter and biased amplifier used for signal processing. For this system the instrument response time is ∼35 ps. Fluorescence was collected at 0°, 54.7°, and 90° with respect to the vertically polarized excitation pulse.

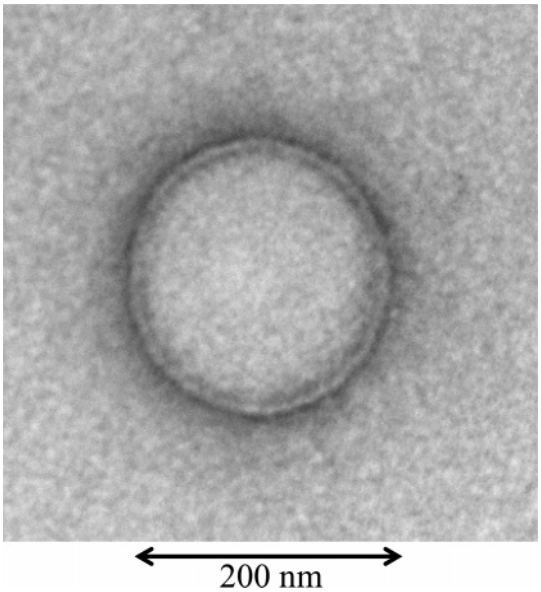

Figure 1. TEM image of unilamellar vesicles produced by extrusion. The average vesicle size is 109 ± 28 nm based on 25 individual determinations.

Transmission Electron Microscopy. Samples were fixed with a 2% osmium tetroxide solution in 0.1 M cacodylate buffer (pH ∼7.4). TEM images (Figure 1) were acquired using a JEOL 100CX TEM operated at an accelerating voltage of 100 kV. The TEM data reveal an average vesicle size of 109 ± 28 nm based on 25 individual determinations.

Background

In this section, we consider the theoretical framework within which we interpret time-resolved fluorescence anisotropy and molecular reorientation data for either one- or two-photon excitation. For either mode of excitation, we monitor emission from the S_1 state of the NBDHA chromophore. While the treatment of fluorescence anisotropy data has been reported elsewhere,[16−19] we believe it is important to provide a brief discussion of this subject to facilitate the interpretation of our experimental data. We start with a discussion of molecular reorientation data acquired using one-photon excitation.

One-Photon Excited Fluorescence Anisotropy. For one-photon excitation, the exciting pulse is polarized vertically and fluorescence transients are collected at 90° with respect to the excitation axis, at polarizations parallel (vertical) and perpendicular (horizontal) to the excitation polarization. These raw data are combined according to eq 1 to generate the induced orientational anisotropy function, $R(t)$ (eq 1)

$$R(t) = \frac{I_{\parallel}(t) - I_{\perp}(t)}{I_{\parallel}(t) + 2I_{\perp}(t)} \tag{1}$$

The chemically important information contained in $R(t)$ is

manifested in the number of exponential decays recovered, their relative fractional contribution, and the time constant(s) of the decay(s). While $R(t)$ can contain up to five exponential decays, the most common case is for a one-component decay, with a two-component decay being observed under certain circumstances. The zero-time value(s) of $R(t)$ range from -0.2 to 0.4 for one-photon excitation, depending on the angle between the excited and emitting transition dipole moments.

The relationship between the decay functionality of $R(t)$ and molecular properties including the rotational diffusion constants and the angle between the excited and emitting transition dipole moments was described by Chuang and Eisenthal.[16] That treatment considers the functional form of $R(t)$ for an arbitrary ellipsoid of rotation, with limiting cases of either an oblate or prolate ellipsoid being used to simplify the general expression for $R(t)$. Judicious assignment of Cartesian axes to the rotating molecule can serve to simplify the functionality of $R(t)$. Generally, the excited transition dipole moment is taken as the x-axis, and for nominally planar molecules such as NBD the π-system defines the $x-y$ plane. For an oblate rotor, $D_z \neq D_x = D_y$, and for a prolate rotor $D_x \neq D_y = D_z$.[16,18,19] For excitation and emission transition dipole moments aligned parallel to one another and along the long (x) axis, $R(t)$ decays according to eqs 2

oblate

$$R(t) = \left(\frac{1}{10}\right)\exp(-(2D_x + 4D_z)t) + \left(\frac{3}{10}\right)\exp(-6D_x t)$$

prolate

$$R(t) = \left(\frac{4}{10}\right)\exp(-6D_z t) \qquad (2)$$

If the transition moments are oriented along the z-axis, an oblate rotor will decay as a single exponential with an exponential term of $(4D_x + 2D_z)$.[16,18−20] These various possibilities have been treated elsewhere in detail, and for the outwardly simple case of a single-exponential decay, there can be ambiguity in resolving the Cartesian components of D.[16] For this reason, we have also measured the induced orientational anisotropy function of NBDHA using two-photon excitation. While the essential physics of molecular motion remain the same regardless of the excitation mechanism, the means by which the initial anisotropic distribution is excited can have a profound influence on the functional form of the resulting fluorescence transients. By comparing the experimental data for one- and two-photon excitation, we obtain a more complete and less ambiguous picture of the rotational diffusion constant for NBDHA in the various environments which we examine.

Two-Photon Excited Fluorescence Anisotropy. Reorientation dynamics probed by two photon excited fluorescence can, in principle, provide more detailed, or at least complementary information on the rotational motion that characterizes NBDHA in solution. We are interested in using two-photon excitation because it is a nonlinear process and thus provides selective excitation of the chromophore of interest without unwanted background absorption that can give rise to heating in thermally sensitive materials or in fragile biological systems. In our discussion of two-photon excited fluorescence anisotropy data, we follow the treatment put forth by the Johnson group.[21−23] Our goal is to relate the two-photon excited anisotropy decays of NBDHA in selected environments to the Cartesian components of its rotational diffusion constant.

Two-photon absorption is a third-order nonlinear process, where two photons from the same incident electric field are absorbed simultaneously. Two-photon absorption is not an efficient process, and measuring the attenuation of the incident electric field is not a practical means of detection. Typically, for two-photon resonant excitation, the population placed in an excited electronic state as a result of two-photon absorption relaxes by internal conversion to the S_1 state, where subsequent radiative decay is detected. The components of the molecular hyperpolarizability that can be accessed by the incident electric field(s) are represented by a tensor[21−24]

$$S = \begin{bmatrix} S_{xx} & S_{xy} & S_{xz} \\ S_{yx} & S_{yy} & S_{yz} \\ S_{zx} & S_{zy} & S_{zz} \end{bmatrix}$$

For most planar chromophores such as NBD, a limited number of tensor elements contribute to two-photon absorption, which are typically written as a 2×2 tensor, containing only S_{xx}, S_{xy} $(=S_{yx})$ and S_{yy}.[21−24] We are interested primarily in the *relative* values of the tensor elements S_{xx} and S_{xy}, and thus normalize these values to $S_{yy} = 1$.

Two-photon excitation provides information on the Cartesian components of the rotational diffusion constant of a chromophore that is complementary to that available from one-photon excitation measurements. Because the details of the orientational anisotropy relaxation depend both on the shape of the initial photoselected anisotropic population and on the two photon tensor elements accessed, the functional form of the anisotropy decay will depend on whether circularly or plane-polarized light was used for two-photon excitation. The anisotropy functions generated from the linearly ($r_1(t)$) and circularly ($r_2(t)$) polarized light are given by

$$r_1(t) = \frac{I_{||}^{\text{linear}}(t) - I_{\perp}^{\text{linear}}(t)}{I_{||}^{\text{linear}}(t) + 2I_{\perp}^{\text{linear}}(t)}$$

$$r_2(t) = \frac{I_{||}^{\text{circular}}(t) - I_{\perp}^{\text{circular}}(t)}{2I_{||}^{\text{circular}}(t) + I_{\perp}^{\text{circular}}(t)} \qquad (3)$$

Both zero-time anisotropies and anisotropy decay time constants are recovered from the experimental data. For both excitation polarizations, the transient anisotropy decays are characterized by the same two time constants, τ_0 and τ_2, each weighted according to the spectroscopic properties of the chromophores. The zero-time anisotropies for these two different excitation polarizations are related to the two-photon tensor elements according to eq 4, for systems where S_{xx}, S_{xy} $(=S_{yx})$ and S_{yy} are the dominant elements.[21−23]

$$r_1(0) = \frac{1}{7}\frac{2(S_{xx} + S_{yy})^2 + (S_{xx} - S_{yy})^2 + 4S_{xy}^2 + 9(S_{xx}^2 - S_{yy}^2)}{2(S_{xx} + S_{yy})^2 + (S_{xx} - S_{yy})^2 + 4S_{xy}^2}$$

$$r_2(0) = \frac{1}{7}\frac{3(S_{xx} - S_{yy})^2 - (S_{xx} + S_{yy})^2 + 12S_{xy}^2 + 6(S_{xx}^2 - S_{yy}^2)}{(S_{xx} + S_{yy})^2 + 3(S_{xx} - S_{yy})^2 + 12S_{xy}^2} \qquad (4)$$

Knowing the experimental values of $r_1(0)$ and $r_2(0)$, we can determine the relative values of S_{xx} and S_{xy} when S_{yy} is normalized to unity. Because we are concerned with the relative values of the tensor elements and not their absolute magnitudes, normalization of the tensor elements to S_{yy} does not reduce the relevant information content of our measurements.

Rotational diffusion will rerandomize the initially anisotropic orientational distribution of the emitting molecules according to eqs 5[21−23]

$$r_1(t) = r_1(0)[c_0 \exp(-t/\tau_0) + c_2 \exp(-t/\tau_2)]$$

$$r_2(t) = r_2(0)[d_0 \exp(-t/\tau_0) + d_2 \exp(-t/\tau_2)] \quad (5)$$

where τ_0 and τ_2 are two different relaxation time constants. The relative contribution of the two time constants is given by the prefactors c_i and d_i, which are in turn related to the rotational diffusion constant and the two-photon tensor elements, as described in eqs 6−10[21−23]

$$c_0 = \frac{(\sqrt{3}a + b)[3(\sqrt{3}a + b)S_{xx}^2 + 3(-\sqrt{3}a + b)S_{yy}^2 + 2bS_{xx}S_{yy} + 4bS_{xy}^2]}{7N^2(3S_{xx}^2 + 3S_{yy}^2 + 2S_{xx}S_{yy} + 4S_{xy}^2)} \quad (6)$$

$$c_2 = \frac{(a - \sqrt{3}b)[3(a - \sqrt{3}b)S_{xx}^2 + 3(a + \sqrt{3}b)S_{yy}^2 + 2aS_{xx}S_{yy} + 4aS_{xy}^2]}{7N^2(3S_{xx}^2 + 3S_{yy}^2 + 2S_{xx}S_{yy} + 4S_{xy}^2)} \quad (7)$$

$$d_0 = \frac{(\sqrt{3}a + b)[(\sqrt{3}a + b)S_{xx}^2 + (-\sqrt{3}a + b)S_{yy}^2 - 4bS_{xx}S_{yy} + 6bS_{xy}^2]}{14N^2(S_{xx}^2 + S_{yy}^2 - S_{xx}S_{yy} + 3S_{xy}^2)} \quad (8)$$

$$d_2 = \frac{(a - \sqrt{3}b)[(a - \sqrt{3}b)S_{xx}^2 + (a + \sqrt{3}b)S_{yy}^2 - 4aS_{xx}S_{yy} + 6aS_{xy}^2]}{14N^2(S_{xx}^2 + S_{yy}^2 - S_{xx}S_{yy} + 3S_{xy}^2)} \quad (9)$$

The relative amplitudes of the decay time constants will provide information about the values of the Cartesian components of the rotational diffusion constant. The parameters a, b, N, and Δ are related to the diffusion constant by

$$a = \sqrt{3}\,(D_y - D_x)$$

$$b = 2D_z - D_y - D_x + 2\Delta$$

$$N^2 = a^2 + b^2$$

$$\Delta = (D_x^2 + D_y^2 + D_z^2 - D_xD_y - D_yD_z - D_xD_z)^{1/2} \quad (10)$$

We use these relationships[16,18,20] and those developed by Johnson and co-workers[21−23] to treat our two-photon excited fluorescence anisotropy data on NBDHA in solvents and unilamellar vesicle structures.

Equations 5 indicate that the two-photon anisotropy decay should exhibit two exponential components, and our experimental data yield single exponential decays in all cases (vide infra). This result has been observed previously,[21] and obtains under the condition that the experimental time constants are similar, with the single time constant representing a weighted average of the two decay time constants. As is the case for Chuang and Eisenthal's treatment, invoking ellipsoidal rotor shapes for reorientation can serve to simplify the form of the expressions for the decay time constants τ_0 and τ_2. Our experimental data for one-photon excitation suggest that NBD reorients as a prolate rotor, $D_x \neq D_y = D_z$ (vide infra), and we apply this effective rotor shape to the equations for τ_0 and τ_2. The equations derived by the Johnson group[21−23] can be simplified to yield

$$\tau_{r1}^{\mathrm{PRO}} = \frac{S_{xx}^2(7D_x + 17D_z) - 4S_{yy}^2(2D_x - D_z) + (S_{xx}S_{yy} + 2S_{xy}^2)\left(\frac{3(D_z^2 + 2D_zD_x)}{2D_x + D_z} + 4D_x - D_z\right)}{8(D_z^2 + 2D_xD_z)(6S_{xx}^2 - 3S_{yy}^2 + S_{xx}S_{yy} + 2S_{xy}^2)} \quad (11)$$

$$\tau_{r2}^{\mathrm{PRO}} = \frac{8S_{xx}^2(2D_x + D_z) - 4S_{yy}^2(2D_x - D_z) - (2S_{xx}S_{yy} + 3S_{xy}^2)\left(6D_x - 5D_z + \frac{9(D_z^2 + 2D_zD_x)}{2D_x + D_z}\right)}{24(D_z^2 + 2D_xD_z)(2S_{xx}^2 - S_{yy}^2 - 2S_{xx}S_{yy} + 3S_{xy}^2)} \quad (12)$$

The various factors that contribute to the two-photon excited anisotropy decay time constants are not related in an intuitive manner to the rotational motion of the molecule, in contrast to the time constant(s) recovered for one-photon excitation. Treating NBD as a prolate rotor, we can determine D_z (eqs 2) and D_x (eq 13)

$$D_x = \frac{17S_{xx}^2D_z + 12S_{xy}^2D_z + 2S_{xx}D_z - 48\tau_1S_{xx}^2D_z^2 - 16\tau_1S_{xy}^2D_z^2 - 8\tau_1S_{xx}D_z + 24\tau_1D_z^2}{7S_{xx}^2 + 4S_{xx} - 96\tau_1S_{xx}^2D_z - 32\tau_1S_{xy}^2D_z - 16S_{xx}D_z\tau_1 + 48\tau_1D_z} \quad (13)$$

We use this information to advantage in probing the immediate environment of NBDHA in a series of solvent and unilamellar vesicle systems of varying composition.

Results and Discussion

As noted in the Introduction, we are interested in understanding the motional dynamics of the chromophore NBDHA both in neat solvents and in the presence of unilamellar vesicles. The issues of primary concern are obtaining a detailed understanding of the dynamics of this chromophore, and whether it localizes to specific region(s) within the unilamellar vesicle structures. We consider first the dynamics of NBDHA in selected neat solvents. Previous literature reports have demonstrated that the polarity of the environment surrounding the NBD chromophore plays a significant role in determining its fluorescence lifetime.[5−10] Our data are consistent with these previous results,[6−8,10] showing a decrease in fluorescence lifetime of NBDHA with increasing solvent polarity. The excited-state population decay of NBDHA is single exponential in all cases, consistent with the expected first-order dynamics of a single emitting species. Fluorescence lifetimes of NBDHA in neat solvents are between 6 and 10 ns. The lifetime values determined by one-photon and two-photon excitation are the same to within the experimental uncertainty, which is expected because radiative emission originates from the same excited electronic state for both modes of excitation. It is difficult to extract detailed chemical information from fluorescence lifetimes because of the system-specific nature of such data and the absence of a comprehensive theoretical framework relating excited-state lifetime to either local environment or molecular properties for systems where the emission bands experience significant inhomogeneous broadening.

For these reasons, we turn to the information available from fluorescence anisotropy data. For NBDHA in neat solvents, the one-photon excited fluorescence anisotropy decays are single exponential. On the basis of Chuang and Eisenthal's treatment, as indicated in eq 2, the single-exponential decay of $R(t)$ indicates that NBDHA is a prolate rotor with $\tau = 1/(6D_z)$.[16,20] The one-photon reorientation times we recover are related

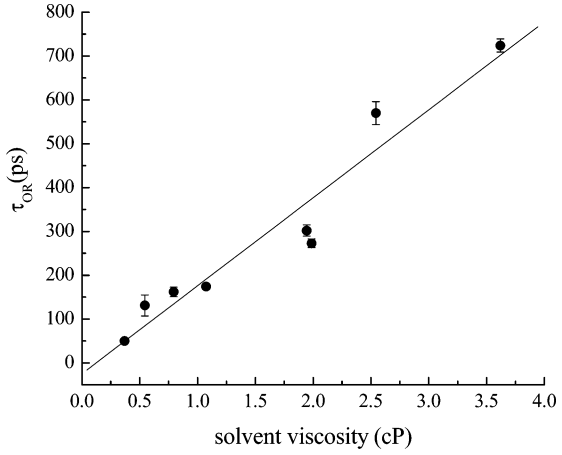

Figure 2. Dependence of NBDHA one-photon excited reorientation time constant on solvent viscosity. The slope of the best-fit line is used to extract the viscosity dependence of the rotational diffusion constant D_z.

directly to the viscosity of the local medium, as described by the modified Debye−Stokes−Einstein (DSE) equation[16,18−20]

$$\tau_{OR} = \frac{\eta V f}{k_B T S} \tag{14}$$

where η is the solvent bulk viscosity, V is the solute hydrodynamic volume $V_{NBDHA} = 245$ Å^3,[25] f is the frictional solvent−solute boundary condition, and S is the solute shape factor. We show in Figure 2 the dependence of τ_{OR} on solvent bulk viscosity, and from those data we determine that $D_z/\eta = 877 \pm 51$ MHz/cP. Despite this useful relationship, there remains the potential ambiguity in determining the Cartesian components of D based on the axis along which the excited transition moment is oriented. We are thus in need of achieving a more thorough understanding of the motional dynamics of NBDHA. In an attempt to lift this ambiguity, we have performed measurements of the transient fluorescence anisotropy of NBDHA for two-photon excitation.

For the reorientation data acquired using two-photon excitation, the recovered anisotropy decay times are not related to the viscosity of the local medium in the same manner as the data for one-photon excitation but are a permutation of D_z, D_x, and the two-photon tensor elements. The one-photon anisotropy data for NBDHA suggest that this chromophore reorients as a prolate rotor in the neat solvents we have studied. It is also possible, under certain circumstances, that the one-photon data could be consistent with the behavior of an oblate rotor, depending on the orientation of the transition dipole moments relative to the dominant rotor axis. In an effort to resolve this potential ambiguity and determine whether NBDHA reorients as a prolate rotor or an oblate rotor, we have treated the two-photon data assuming both rotor shapes. Assuming an oblate rotor shape yields physically unrealistic, negative values for D_x and D_z that are not consistent between the one-photon and two-photon data. On the basis of these findings, we assert that NBDHA reorients as a prolate rotor in the neat solvents we have studied. We report the values of D_z and D_x in the solvents used here in Table 1. These data show that the ratio of diffusion coefficients is $D_z/D_x \sim 2$ for all solvents, a result that is possible only by comparing the two independent data sets, analogous to the information extracted from anisotropy measurements on Rhodamine 640 when excited to two different initial electronic states.[26]

TABLE 1: Solvent-dependence of D_z and D_x for NBDHA in Neat Solvents

solvent	viscosity (cP)	D_z (MHz)	D_x (MHz)	D_z/D_x
acetonitrile	0.369	3370 ± 6	1887 ± 1	2.1
methanol	0.544	1270 ± 18	610 ± 1	1.7
DMF	0.794	1030 ± 7	599 ± 1	1.7
ethanol	1.074	960 ± 3	566 ± 1	1.8
propanol	1.945	550 ± 4	324 ± 1	1.8
DMSO	1.987	610 ± 4	352 ± 1	1.7
butanol	2.544	290 ± 5	165 ± 1	1.7
pentanol	3.619	230 ± 2	128 ± 1	1.8

With this information in hand, we now have a relevant framework within which to evaluate the behavior of NBDHA in the presence of unilamellar vesicles. We have synthesized unilamellar vesicles from solutions containing 10^{-4} M NBDHA. A variety of unilamellar vesicle compositions were used to determine whether the NBDHA chromophore functions as a sensor of vesicle structure and composition. The addition of cholesterol and sphingomyelin to phospholipid vesicle structures is known to induce phase-segregated regions within the bilayer structures.[2−4] Ongoing work in the Blanchard laboratory shows that varying the composition of bilayers does, in fact, influence the dynamics of the constituents.[27] Those results were obtained using chromophores tethered to specific bilayer constituents such as cholesterol or a phospholipid, and they thus provided information on the region(s) of interest within the bilayer structure. A central goal of this work is to determine whether the NBDHA chromophore locates within specific vesicle regions. The underlying question is the structural homology required of a probe molecule in order for it to locate within specific regions of the bilayer.

To help understand the location of NBDHA in vesicle systems, we consider first the fluorescence lifetime of this chromophore. As noted earlier, there is limited information available from fluorescence lifetime measurements by themselves, but when such data are compared to NBDHA lifetimes in other systems, it is possible to garner some useful environmental insight. For each vesicle system, the NBDHA excited state lifetime decays exhibited a single exponential functionality. Previous literature reports have shown that the fluorescence lifetime of NBD in an aqueous or polar environment is typically subnanosecond,[6,7,9,10] suggestive of strong interactions between solvent and solute, such as hydrogen bonding and dipolar coupling. We note that there is evidence in the literature for direct chromophore−chromophore interactions between NBD moieties under certain experimental conditions.[11] Given both the functionality and time constant of the lifetime data we recover for our systems, we do not believe that chromophore dimers contribute significantly to our results. We recover the interesting result that, regardless of vesicle composition, the NBDHA lifetimes are all ca. 1 ns, suggesting that the environment sensed by the NBDHA chromophore is of similar polarity in all cases. If this explanation is true, the steady-state fluorescence spectra of NBDHA should be similar for all systems, and we consider these data next.

The steady-state spectra of NBDHA in vesicles and in water are shown in Figure 3. The NBDHA absorption band maximum and shape are substantially different in water than in vesicle-containing solutions. The absorption maximum for NBDHA in vesicle-containing solutions is ∼475 nm and is centered at ∼484 nm in water. We conclude from these data that NBDHA is not in the aqueous phase in vesicle-containing solutions. The chromophore NBD is known to have a fluorescence quantum yield that depends sensitively on the polarity of its environment. In water, NBD has a low quantum yield,[7,8] and in our

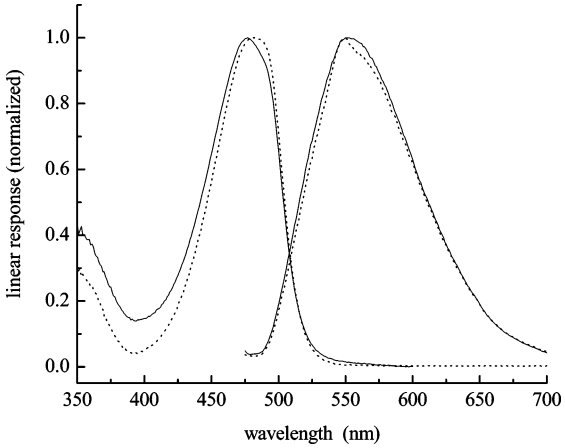

Figure 3. Normalized absorption and emission spectra of NBDHA in neat water (dashed line) and in a solution containing DLPC vesicles (solid line). Spectra for all vesicle-containing solutions were identical.

measurements of NBDHA we were unable to detect a significant time-resolved fluorescence signal in water. On the basis of both the steady state absorption data and the time-resolved emission data, it is clear that in vesicle-containing solutions, NBDHA does not reside in the bulk water region of this system and that for all vesicle-containing solutions the chromophore senses essentially the same environment.

We consider next the information content of the reorientation data for NBDHA in vesicle-containing solutions. When considering anisotropy decays for NBDHA in the presence of vesicles, we have to decide on the most appropriate model to use in interpreting these data. Depending on where in the solution the chromophore resides, either the DSE (free rotor, eq 14) model[28−30] or the hindered rotor model[31−33] could be used to interpret the data. The hindered rotor model has previously been used to describe the motion of a chromophore embedded in a membrane and must be considered here based on the steady-state absorption data. In this model, the motion of a chromophore is restricted by its environment, which is modeled as a cone. The cone angle that characterizes the chromophore motional freedom is related to the measured time constant of the anisotropy decay according to

$$\tau = \frac{7\theta_o^{\,2}}{24D_w} \tag{15}$$

The time constant associated with motional relaxation of the chromophore is not determined unambiguously because of the dependence of this quantity both on the cone angle in which the chromophore is free to move and on the "wobbling" diffusion constant of the chromophore as it moves about its bond to its anchoring functionality. We note that in this model the measured time constant behaves differently than the quantity τ_{OR} (eq 14), which is measured for a free chromophore in solution. For the hindered rotor, the anisotropy decay time τ scales with the cone angle swept out. For a restrictive environment (small θ_0), a rapid time constant is measured because the chromophore samples a small volume, and for a relatively free environment (large θ_0), τ is long because of the comparatively greater volume the chromophore has access to. In contrast, for a free rotor, a fast time constant τ_{OR} is reflective of a low viscosity environment and a slow time constant implies a high viscosity, restrictive environment. Also, for hindered rotors, the anisotropy does not decay to zero at $t = \infty$ as it does in bulk solutions, because a restricted range of motional freedom is available to the chromophore. In principle, the observation of a nonzero $R(\infty)$ value would indicate that the hindered rotor is the appropriate model. Because we are using vesicles, however, and restriction in the orientational distribution associated with chromophore confinement within the bilayer is orientationally averaged over 4π steradians macroscopically owing to the spherical shape of the vesicles, $R(\infty) = 0$ for all measurements. The choice of the model most appropriate for the interpretation of our data must therefore be made based on other factors.

We consider that, if NBDHA were bound to the surface of the unilamellar vesicles, it would enjoy substantial motional freedom. We make this structural argument based on the fact that, for the lipids we use, there is a cationic quaternary ammonium species in closest proximity to the water at the lipid−solution interface. Because we make our measurements at pH 8, the NBDHA is fully deprotonated (precluding carboxylic acid tail-to-tail chromophore dimer formation), and if the chromophore were to interact with the vesicle, as suggested by the steady state absorption data, an ionic interaction would be possible. In this picture, the nominally tethered chromophore would experience a cone angle of $2\theta_0 \sim 180°$, which is a limiting case that renders the chromophore equivalent to a free rotor. Also, the strength of the ionic interaction postulated above would be on the order of several kcal/mol at most, and the persistence time for such interactions would be on the order of hundreds of picoseconds. For both of these reasons, we assert that our reorientation data for NBDHA in the presence of vesicles are best understood in the context of the free rotor model rather than the hindered rotor model.

Interpreting our reorientation data within the framework of the free rotor model yields the result that NBDHA reorients as a prolate rotor in the presence of vesicles, qualitatively the same as for its behavior in neat solvents. We have synthesized vesicles in a range of compositions, including the use of two different lipids with melting points substantially below (DLPC, mp = −1 °C) and substantially above (DSPC, mp = 55 °C) room temperature, and with the addition of cholesterol and sphingomyelin. These different vesicle compositions are known to produce phase-segregated bilayer structures, and the local environments created by these different phases vary widely in both their polarity and rigidity.[2−4,34] Despite the wide range of environments within the vesicles that are available to NBDHA, we recover essentially the same one-photon-excited reorientation times, regardless of vesicle composition (Table 2, Figure 4). While there may be some slight variation between individual systems, these differences are barely different from the experimental uncertainty. For this reason we do not attempt to provide any more detailed, system-dependent interpretation of these values. We also note that, while the two-photon-excited anisotropy decays produce different time constants than those seen for the one-photon data, as expected, the same behavior is seen for all of the anisotropy decay time data sets.

Treatment of the one-photon-excited anisotropy decay times of NBDHA in vesicle-containing solutions in the context of a free rotor allows τ_{OR} to be related to the viscosity of the environment through the DSE equation (eq 14), and the observation of single-exponential anisotropy decays allows assignment of a prolate rotor shape to NBDHA in the presence of vesicles, based on our measurements of NBDHA in neat solvents (vide supra). Comparing the reorientation times of NBDHA in vesicle-containing solutions to the same data for NBDHA in neat solvents indicates that the local environment of NBDHA is characterized by a viscosity of ∼1 cP, a value fully consistent with an aqueous environment. These data, taken

TABLE 2: Dependence of NBDHA One- and Two-Photon-Excited Anisotropy Decay Time Constants on Vesicle Composition[a]

vesicle system	τ_{OR} (one photon, ps)	τ_{linear} (two photon, ps)	$\tau_{circular}$ (two photon, ps)	τ_{fl} (ps)	D_z/D_x
DLPC	163 ± 10	121 ± 5	102 ± 14	1173 ± 88	1.8
DLPC/chol	166 ± 4	127 ± 5	95 ± 4	1168 ± 66	1.8
DLPC/chol/spm	194 ± 5	132 ± 19	106 ± 16	1177 ± 62	1.7
DSPC	186 ± 6	126 ± 8	97 ± 9	1144 ± 45	1.8
DSPC/chol	176 ± 6	109 ± 6	107 ± 10	1132 ± 23	1.7
DSPC/chol/spm	165 ± 4	122 ± 4	97 ± 10	1145 ± 44	1.7
DLPC/DSPC	159 ± 6	125 ± 5	102 ± 4	1157 ± 48	1.9
DLPC/DSPC/chol	161 ± 8	126 ± 8	89 ± 9	1147 ± 40	1.7
DLPC/DSPC/chol/spm	186 ± 5	87 ± 2	75 ± 5	1067 ± 41	2.0

[a] Abbreviations: DLPC = 1,2-dilauroyl-*sn*-glycero-3-phosphocholine; DSPC = 1,2-distearoyl-*sn*-glycero-3-phosphocholine; chol = cholesterol; spm = sphingomyelin.

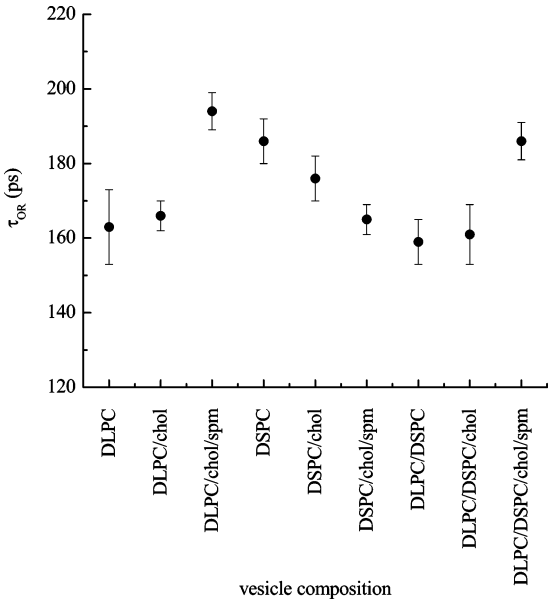

Figure 4. Dependence of NBDHA reorientation on vesicle composition.

in conjunction with the steady-state data (Figure 3), suggest that the probe resides in the polar headgroup region, in the immediate vicinity of the bilayer.

The two-photon-excited anisotropy decays for NBDHA in solvents were modeled as both a prolate and an oblate rotor to determine which model provided results that were consistent with the one-photon data. We have treated the two-photon data for NBDHA in vesicle-containing solution the same way, and the results of this treatment are that a self-consistent result is obtained only if NBDHA is modeled as a prolate rotor. For the two-photon-excited anisotropy data, single exponential decays are seen, and the reorientation times for all systems are the same for both linearly and circularly polarized excitation, regardless of vesicle composition. We apply eq 13 to our data to extract the quantity D_x. Combining the two-photon and the one-photon data we recover a ratio $D_z/D_x \sim 2$ (Table 2), the same ratio that we determined for NBDHA in neat solvents. The consistency of the results between the two different types of environments argues for the applicability of the free rotor model for the interpretation of NBDHA molecular motion in vesicle-containing solutions.

We note that it is, in principle, possible for the NBDHA chromophore to be incorporated to a limited extent (shallow incorporation) into the bilayer structure, and under this condition it would sense a polar environment that is likely not too different than that of bulk water.[35−38] We believe that the reorientation data we have presented allow us to distinguish between the possibility of shallow incorporation and the chromophore being at the bilayer interface. If the chromophore were incorporated to any significant extent within the bilayer structure, the ratio of D_z/D_x would be altered by virtue of its spatial confinement. We find experimentally that the ratio D_z/D_x for NBDHA in vesicle-containing solutions is the same as that in neat liquid solvents, indicating that it resides in an environment that affords substantial orientational freedom that varies very little if at all with bilayer composition. The only environment that fits these criteria fully is the interface between the bilayer and the bulk liquid.

Conclusions

We have studied the steady-state and time-resolved optical properties of the chromophore NBDHA in a series of neat solvents and in vesicle-containing solutions. We have used both one-photon excitation and two-photon excitation for our anisotropy measurements, and analyzing these data to find a self-consistent solution allows us to determine that the chromophore reorients as a prolate rotor with $D_z/D_x \sim 2$ in all cases. For NBDHA in vesicle-containing solutions, we observe reorientation dynamics that are independent of vesicle composition, even though the steady-state absorption and fluorescence lifetime data on these systems indicate that the chromophore does not reside in a purely aqueous environment. The location of the NBDHA chromophore that is most consistent with the entire body of steady-state and time-resolved emission data is that the chromophore resides at the bilayer−solution interface, near the zwitterionic phosphocholine headgroups. In this region, interactions between the headgroups and the NBDHA are possible. All solutions are at pH ∼8; therefore the NBDHA is essentially all deprotonated, allowing ionic interactions to dominate in this system. The larger implication of this work is that there needs to be a very close match between chromophore side group functionality and a bilayer constituent for there to be incorporation into specific regions of the bilayer structures. We do note that the chromophore interaction with the vesicles is selective for the phospholipid regions, but in a way that is not sensitive to any lipid local organization.

Acknowledgment. We are grateful to the National Science Foundation for support of this work through Grant CHE 0445492.

References and Notes

(1) Simons, K.; van Meer, G. *Biochemistry* **1988**, *27*, 6197.
(2) Crane, J. M.; Tamm, L. K. *Biophys. J.* **2004**, *86*, 2965.
(3) Hao, M.; Maxfield, F. R. *J. Fluoresc.* **2001**, *11*, 287.
(4) Scherfeld, D.; Kahya, N.; Schwille, P. *Biophys. J.* **2003**, *85*, 3758.
(5) Chapman, C. F.; Liu, Y.; Sonek, G. J.; Tromberg, B. J. *Photochem. Photobiol.* **1995**, *62*, 416.

(6) Chattopadhyay, A.; London, E. *Biochim. Biophys. Acta* **1988**, *938*, 24.
(7) Fery-Forgues, S.; Fayet, J.-P.; Lopez, A. *J. Photochem. Photobiol., A* **1993**, *70*, 229.
(8) Lin, S.; Struve, W. S. *Photochem. Photobiol.* **1991**, *54*, 361.
(9) Mazeres, S.; Schram, V.; Tocanne, J.-F.; Lopez, A. *Biophys. J.* **1996**, *71*, 327.
(10) Mukherjee, S.; Chattopadhyay, A.; Samanta, A.; Soujanya, T. *J. Phys. Chem.* **1994**, *98*, 2809.
(11) Tsukanova, V.; Grainger, D. W.; Salesse, C. *Langmuir* **2002**, *18*, 5539.
(12) Hunter, D. G.; Frisken, B. J. *Biophys. J.* **1998**, *74*, 2996.
(13) Johnson, J. M.; Ha, T.; Chu, S.; Boxer, S. G. *Biophys. J.* **2002**, *83*, 3371.
(14) Moscho, A.; Orwar, O.; Chiu, D. T.; Modi, B. P.; Zare, R. N. *Proc. Natl. Acad. Sci. U.S.A.* **1996**, *93*, 11443.
(15) Patty Philipus, J.; Frisken Barbara, J. *Biophys. J.* **2003**, *85*, 996.
(16) Chuang, T. J.; Eisenthal, K. B. *J. Chem. Phys.* **1972**, *57*, 5094.
(17) Jiang, Y.; Blanchard, G. J. *J. Phys. Chem.* **1994**, *98*, 6436.
(18) Blanchard, G. J. *J. Chem. Phys.* **1987**, *87*, 6802.
(19) McPhie, P. In *Principles of Fluorescence Spectroscopy*, 2nd ed.; Lakowicz, J. R., Ed.; Kluwer Academic/Plenum: New York, 2000; Vol. 287.
(20) Tao, T. Time-dependent fluorescence depolarization and Brownian rotational diffusion coefficients of macromolecules, 1969.
(21) Johnson, C. K.; Wan, C. *Top. Fluoresc. Spectrosc.* **1997**, *5*, 43.
(22) Wan, C.; Johnson, C. K. *Chem. Phys.* **1994**, *179*, 513.
(23) Wan, C.; Johnson, C. K. *J. Chem. Phys.* **1994**, *101*, 10283.
(24) Callis, P. R. *J. Chem. Phys.* **1993**, *99*, 27.
(25) Edward, J. T. *J. Chem. Educ.* **1970**, *47*, 261.
(26) Dela Cruz, J. L.; Blanchard, G. J. *J. Phys. Chem. A* **2001**, *105*, 9328.
(27) Koan, M. M. Private communication.
(28) Debye, P. *Polar Molecules*; Chemical Catalog Co., Inc.: New York, 1929.
(29) Perrin, F. *J. Phys. Radium* **1936**, *7*, 1.
(30) Zwanzig, R.; Harrison, A. K. *J. Chem. Phys.* **1985**, *83*, 5861.
(31) Kinosita, K., Jr.; Ikegami, A.; Kawato, S. *Biophys. J.* **1982**, *37*, 461.
(32) Kinosita, K., Jr.; Kawato, S.; Ikegami, A. *Biophys. J.* **1977**, *20*, 289.
(33) Szabo, A. *J. Chem. Phys.* **1984**, *81*, 150.
(34) Wisniewska, A.; Draus, J.; Subczynski, W. K. *Cell. Mol. Biol. Lett.* **2003**, *8*, 147.
(35) Costa, E. J. X.; Shida, C. S.; Biaggi, M. H.; Ito, A. S.; Lamy-Freund, M. T. *FEBS Lett.* **1997**, *4116*, 103.
(36) Dhanvantari, S.; Arnaoutova, I.; Snell, C. R.; Steinbach, P. J.; Hammond, K.; Caputo, G. A.; London, E.; Loh, Y. P. *Biochemistry* **2002**, *41*, 52.
(37) Drummen, G. P. C.; van Liebergen, L. C. M.; Op den Kamp, J. A. F.; Post, J. A. *Free Radical Biol. Med.* **2002**, *33*, 473.
(38) Lee, S.; Yoshida, M.; Mihara, H.; Aoyagi, H.; Kato, T.; Yamasaki, N. *Biochim. Biophys. Acta* **1989**, *984*, 174.